

Graphene Passively Q-Switched Nd:YAG Laser by 885 nm Laser Diode Resonant Pumping

Liwei Xu ¹, Yingyi Li ¹, Jun Cai ¹, Wanli Zhao ¹, Tongyu Liu ¹, Tongyu Dai ², Youlun Ju ² and Yu Ding ^{1,*}

¹ Science and Technology on Electro-Optical Information Security Control Laboratory, Tianjin 300308, China
² National Key Laboratory of Tunable Laser Technology, Harbin Institute of Technology, Harbin 150001, China
* Correspondence: dingyu_123@outlook.com

Abstract: A graphene passively Q-switched Nd:YAG laser experienced resonant pumping by an 885 nm laser diode (LD), as demonstrated in this paper. In the continuous-wave operation, the maximum average output power was up to 1.8 W with the absorbed pump power being 11.7 W, and the slope efficiency was 51.2%. In the Q-switching operation, the maximum average output power was up to 639 mW with a pulse width of 2.06 μ s at the repetition frequency of 102.7 kHz, while the slope efficiency and the beam quality factor M^2 were 25.3% and 1.25, respectively.

Keywords: Nd:YAG; passively Q-switched; graphene; resonant pumping



Citation: Xu, L.; Li, Y.; Cai, J.; Zhao, W.; Liu, T.; Dai, T.; Ju, Y.; Ding, Y. Graphene Passively Q-Switched Nd:YAG Laser by 885 nm Laser Diode Resonant Pumping. *Appl. Sci.* **2022**, *12*, 8365. <https://doi.org/10.3390/app12168365>

Academic Editor: Edik U. Rafailov

Received: 23 June 2022

Accepted: 16 August 2022

Published: 21 August 2022

Publisher's Note: MDPI stays neutral with regard to jurisdictional claims in published maps and institutional affiliations.



Copyright: © 2022 by the authors. Licensee MDPI, Basel, Switzerland. This article is an open access article distributed under the terms and conditions of the Creative Commons Attribution (CC BY) license (<https://creativecommons.org/licenses/by/4.0/>).

1. Introduction

The 1 μ m passively Q-switched solid-state lasers have a lot of applications such as in wind-finding lidar, remote sensing, material processing and medical diagnosis [1–4]. The most common solid-state laser mediums generated by the 1 μ m lasers are doped with the Nd³⁺ ions. Compared with the other laser mediums doped with Nd³⁺, the Nd:YAG crystal is more suitable for the passively Q-switching operation due to its long upper-level lifetime, high thermal conductivity and low thermal expansion coefficient. At present, the pump wavelengths of the Nd:YAG lasers are the traditional 808 nm and the resonant-pumping 885 nm [5–9]. Although the former is widely used, its thermal effect is very significant under the end-pumping mode. The latter could effectively reduce the thermal effect and increase the output power and the conversion efficiency of the end-pumped laser due to the reduction in quantum loss.

In the 1 μ m passively Q-switched solid-state lasers, the most frequently used saturated absorbers (SA) are the Cr:ZnSe, Cr:YAG [10–12], gold nanomaterials [13–15], semiconductor saturable absorber mirror (SESAM) [16–18] and graphene. Among them, graphene has the properties of a short response time, a fast recovery time, a high transmittance, a high damage threshold, a high thermal conductivity and has excellent optical properties, due to its zero-bandgap structure. Pure non-defective, single-layer graphene with a thermal conductivity of up to 5300 W/m·K and a favorable optical absorption capacity was chosen, independent of optical frequencies and optical conductivity constants. Compared with the Cr:ZnSe and Cr:YAG crystals, graphene has the advantages of better chemical stability and a smaller volume. Compared with gold nanomaterials, graphene is more suitable for long-time operation due to it having a weaker photothermal effect. Compared with SESAM, graphene has a lower cost and lower laser threshold. Moreover, graphene has saturable absorptions in both visible and infrared bands. Therefore, graphene is of great value in the passively Q-switching and mode-locked lasers.

A graphene-based passively Q-switched Nd:YAG laser has been reported in 2010, for which the output power was 105 mW, with the slope efficiency of 1.3% vs. the incident pump power [19]. A graphene-based passively Q-switched Nd:YAG laser for which the single pulse energy was 21.98 μ J at the shortest pulse width of 584 ns has been reported in 2012 [20]. Another graphene-based passively Q-switched Nd:YAG laser has been reported

in 2015, for which the output power was 305 mW, with an optical-optical efficiency of 10.2% versus the incident pump power [21]. In all of the above reports, the traditional pump wavelength of 808 nm was employed.

The end-pumping of an Nd:YAG laser using bonded crystals with different doping concentrations through the use of an 885 nm LD has been reported in 2013, for which the optical-optical efficiency was 23% versus the absorbed pump power in the continuous wave (CW) operation, and the output power was 200 mW in the passively Q-switching operation using the Cr:YAG crystal as the SA [22]. The end-pumping of a passively Q-switched pulse train laser with the composite crystal of YAG-Nd:YAG-Cr:YAG through the use of an 885 nm LD has been reported in 2017, for which the single pulse energy was 239 μJ with a pulse repetition frequency (PRF) of 86.3 kHz [23]. However, the end-resonant-pumping of a passively Q-switched Nd:YAG laser using graphene as the SA through the use of a 885 nm LD, with the advantages of a reduced thermal effect and a higher conversion efficiency, has not been reported yet.

In this paper, we demonstrated a passively Q-switched Nd:YAG laser resonantly pumped by the 885 nm LD using an SA of graphene. In the CW operation, the absorbed pump power was 11.7 W, the average output power was 1.8 W and the slope efficiency was 51.2%, and the maximum average output power was 639 mW, with a pulse width of 2.06 μs and a PRF of 102.7 kHz in the passively Q-switching operation.

2. Experimental Setup

Figure 1 shows the experimental scheme of the passively Q-switched Nd:YAG laser based on inclusion of the graphene. A fiber-coupled LD was employed as the pump, the core diameter and NA of which were 200 μm and 0.22, respectively. The central wavelength and maximum output power of the LD were 885 nm and 175 W, respectively. The dimensions of the Nd:YAG crystal with an Nd^{3+} doping fraction of 0.5% were 40 mm (length) \times 6 mm (width) \times 2 mm (high). The crystal, both cross-sections of which were anti-reflective at 0.8~0.9 μm and 1.0~1.1 μm , was wrapped in the heat sink made of copper and controlled at 15 $^{\circ}\text{C}$ by the thermoelectric cooler. The pump beam converged into the center of the crystal with a radius of 160 μm through the coupling system.

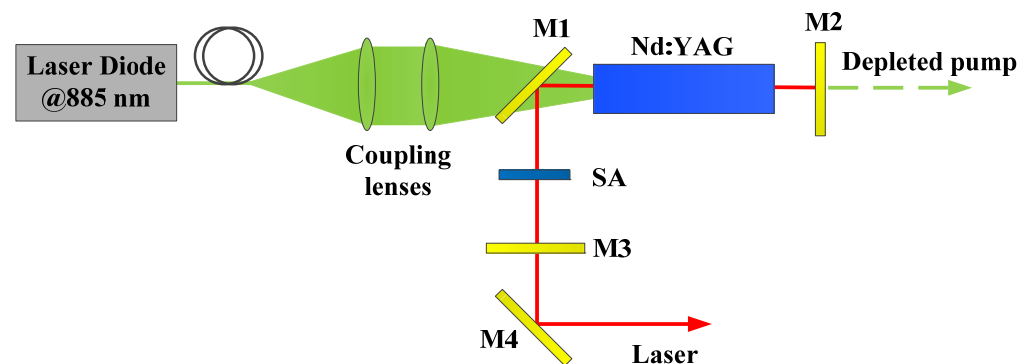


Figure 1. Experimental scheme of the Nd:YAG laser.

The cavity had a L-shaped structure with a physical length of 160 mm. Compared with the straight cavity, the L-shaped cavity could reduce the space and effectively avoid the pump feeding back to the LD. In the device, the distance between the lenses, M1 and M2 was 65 mm, and the distance between M1 and M3 was 95 mm. M1~M4 were all flat mirrors. M1 had high transmittance at 0.8~0.9 μm and high reflectance at 1.0~1.1 μm at an angle of 45 $^{\circ}$; M2 had high transmittance at 0.8~0.9 μm and high reflectance at 1.0~1.1 μm ; M3 had high transmittance at 0.8~0.9 μm and a transmittance of 30% at 1.0~1.1 μm ; M4 had high reflectance at 1.0~1.1 μm at an angle of 45 $^{\circ}$. The graphene was laid between M1 and M3. The substrate of SA was a mirror made of a CaF_2 crystal, and a graphene material that was dissolved in ethanol was coated on one surface of the CaF_2 mirror using a rotary

coater (KW-4A, Chinese Academy of Sciences, Beijing, China). The mirror diameter of the SA was 20 mm, which was a multilayer graphene. The transmittance of the SA at 1.064 μm was measured and found to have been approximately 87.2%.

The absorbed pump power and average output power of the Nd:YAG laser in the CW and Q-switching operation were measured using an Ophir power meter (power range: 20 mW–20 W). The temporal characteristics of the Q-switched Nd:YAG laser were measured using the Si-biased photodetector from Thorlabs, DET025AL/M, and recorded using the oscilloscope from Tektronix MSO 3034.

3. Experimental Results

Figure 2 shows the average output power depending on the absorbed pump power of the Nd:YAG laser in the CW and Q-switching operation. The CW operation was studied first without the graphene. At an absorbed pump power of 11.7 W, the maximum average output power was 1.8 W with a slope efficiency of 51.2%. After the graphene was inserted into the cavity, under the same conditions as the above absorption pump power, the average maximum time output power was 639 mW with a slope efficiency of 25.3% vs. the threshold of 9.21 W. The lines of the output power vs. the absorbed pump power are shown in Figure 2. The equation of the lines is $y = a + bx$, and the R^2 of the lines are 0.99777 and 0.99602, respectively. The instability of the average output power of the Q-switching operation was $\pm 3.1\%$. Compared with the CW operation, during the Q-switching operation, the average output power and the slope efficiency were lower, one possible reason for this was that the graphene increased the intracavity loss.

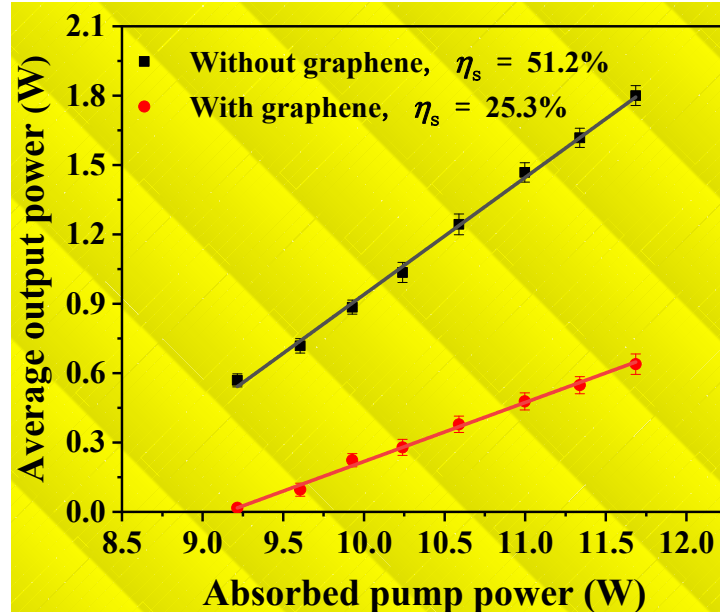


Figure 2. Average output power vs. the absorbed pump power with and without the graphene.

Figure 3 shows the pulse width (full width-half maximum) and PRF depending on the absorbed pump power in the Q-switching operation. When the absorbed power was close to the threshold of 9.21 W, the pulse width was 4.06 μs , and when the absorbed power was 11.7 W, the pulse width reduced to 2.06 μs . The PRF increased from 24.7 kHz to 102.7 kHz, corresponding to the absorbed power of 9.21 W to 11.7 W. The pulse width and PRF depending on the absorbed pump power were approximately linear.

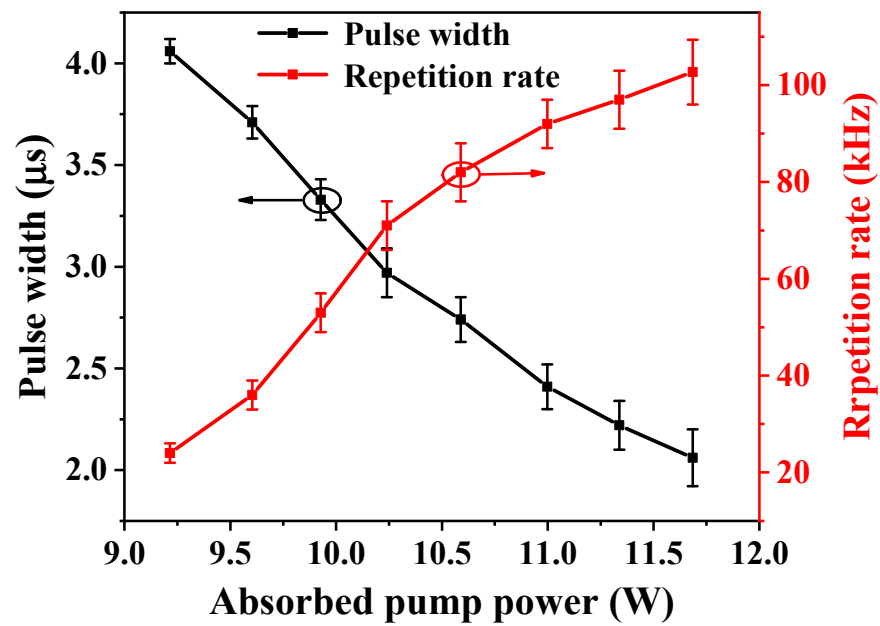


Figure 3. Pulse width and PRF vs. the absorbed pump power.

Figure 4 shows the relationship between the single pulse energy and peak power vs. the absorption pump power. When the absorbed pump power was at its maximum, 11.7 W, the single pulse energy was also at its maximum of 6.2 μJ, corresponding to the peak power of 3 W.

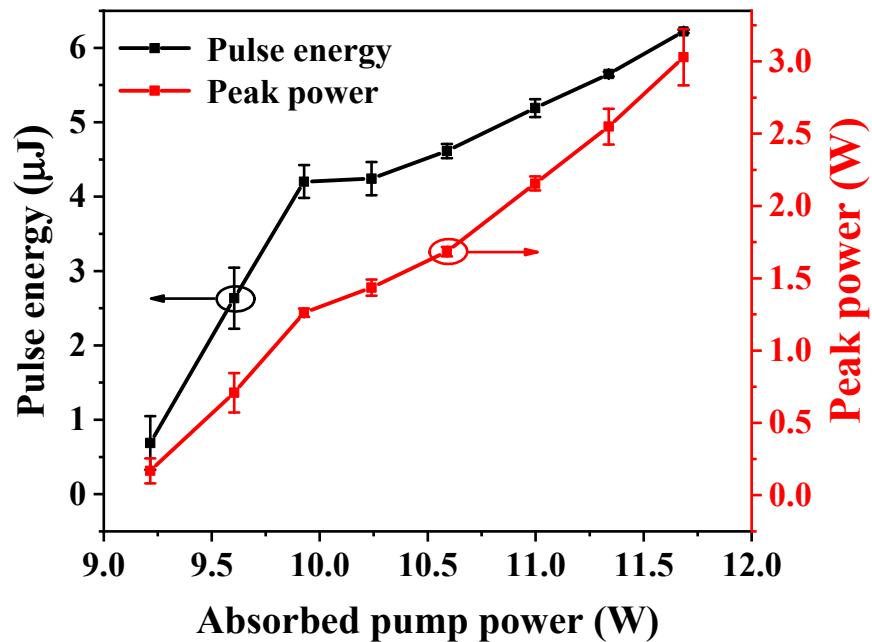


Figure 4. Single pulse energy and peak power vs. the absorbed pump power.

Figure 5 shows the pulse profile when the absorbed pump power reached the threshold. The pulse width was 4.06 μs and the illustration of Figure 5 shows the corresponding pulse sequence. When the absorbed pump power reached 11.7 W, the pulse width decreased to 2.06 μs.

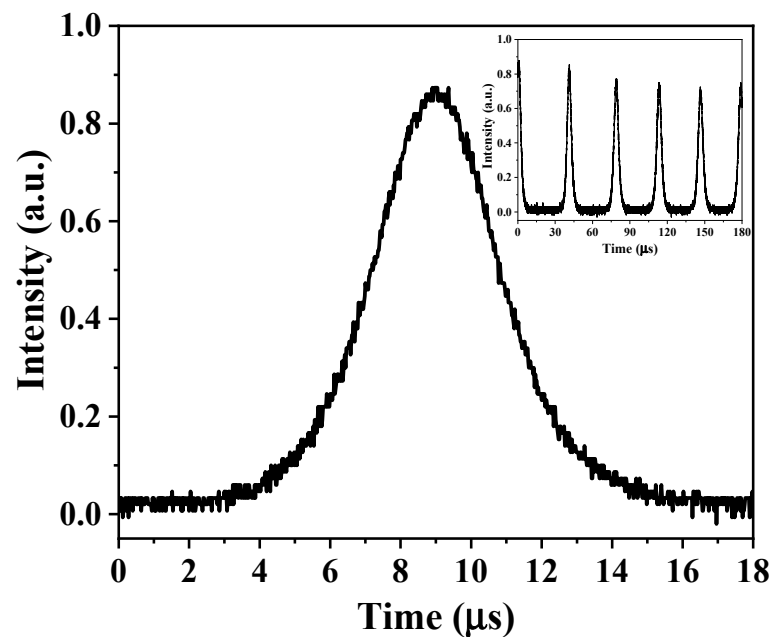


Figure 5. A pulse profile of the threshold pump power. (insert) A pulse sequence of the Q-switched laser.

The beam quality factor, M^2 , in the Q-switching operation was studied at the average output power of 639 mW, taking advantage of the knife-edge method. Figure 6 shows the laser beam radii depending on their location relative to the focal lens, which was used for leading out the waist of the oscillating beam in the cavity. Through Gaussian fitting, the M^2 factors was calculated to be 1.25.

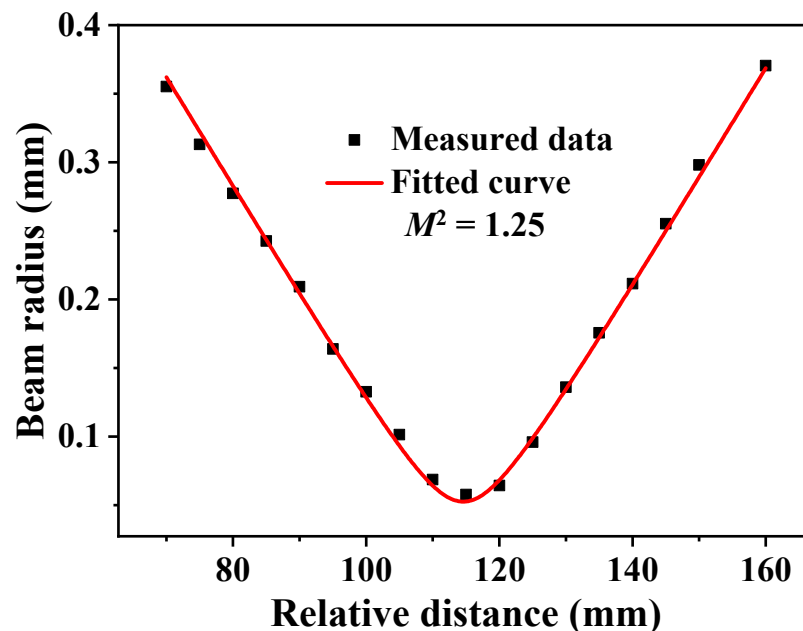


Figure 6. Beam quality of the Q-switched Nd:YAG laser.

4. Conclusions

Taking advantage of the pump of an 885 nm LD and the use of graphene as an SA, a passively Q-switched Nd:YAG laser was demonstrated in this paper. At the absorbed pump power of 11.7 W, the maximum average output power was 1.8 W with a slope efficiency of 51.2% when the SA was absent, and the average output power was decreased to 639 mW with a slope efficiency of 25.3% when the SA was inserted. The pulse width decreased

from 4.06 μs to 2.06 μs , and the PRF increased from 24.7 kHz to 102.7 kHz, corresponding to the absorbed power from 9.21 W to 11.7 W. At the maximum average output power of 639 mW, the M^2 factor was measured to be 1.25 using the knife-edge method. This research demonstrated that the graphene passively Q-switched Nd:YAG laser being pumped by the 885 nm LD is an efficient way to generate radiation with several-microsecond-level pulse width and a hundred-kilohertz-level PRF.

Author Contributions: Conceptualization, L.X. and Y.L.; methodology, L.X.; validation, L.X., Y.L. and Y.D.; investigation, J.C., W.Z. and T.D.; resources, T.L. and Y.J.; data curation, L.X.; writing—original draft preparation, L.X.; writing—review and editing, L.X. and Y.L.; supervision, T.L. and T.D.; project administration, Y.D. All authors have read and agreed to the published version of the manuscript.

Funding: This research received no external funding.

Data Availability Statement: The data presented in this study are available on request from the corresponding author.

Conflicts of Interest: The authors declare no conflict of interest.

References

1. Christian, L.; Oliver, L.; Oliver, R.; Benjamin, W.; Christian, W. Frequency and timing stability of an airborne injection-seeded Nd:YAG laser system for direct-detection wind lidar. *Appl. Opt.* **2017**, *56*, 9057–9068.
2. Liu, D.; Yang, Y.; Zhou, Y.; Huang, H.; Cheng, Z.; Luo, J.; Zhang, Y.; Duan, L.; Shen, Y.; Bai, J.; et al. High spectral resolution lidar for atmosphere remote sensing: A review. *Infrared Laser Eng.* **2015**, *44*, 2535–2546.
3. Hu, Y.; Yao, Z. Overlapping rate effect on laser shock processing of 1045 steel by small spots with Nd:YAG pulsed laser. *Surf. Coat. Technol.* **2008**, *202*, 1517–1525. [[CrossRef](#)]
4. Liu, F.; Hua, Y.; Wu, H.; Gao, Y.; Wu, H. Research progress on soot measurement by laser induced incandescence. *J. Exp. Fluid Mech.* **2017**, *31*, 1–12.
5. Frede, M.; Wilhelm, R.; Kracht, D. 250 W end-pumped Nd:YAG laser with direct pumping into the upper laser level. *Opt. Lett.* **2006**, *31*, 3618–3619. [[CrossRef](#)] [[PubMed](#)]
6. Li, F.; Zhang, X.; Zong, N.; Yang, J.; Peng, Q.; Cui, D.; Xu, Z. High-efficiency High-power Nd:YAG laser under 885 nm laser diode pumping. *Chin. Phys. Lett.* **2009**, *26*, 92–94. [[CrossRef](#)]
7. Zhang, X.; Li, F.; Zong, N.; Le, X.; Cui, D.; Xu, Z. High-efficiency 17 W, 80 MHz repetition rate, passively mode-locked TEM00 Nd:YAG oscillator pumped at 885 nm. *Laser Phys.* **2011**, *21*, 435–438. [[CrossRef](#)]
8. Chang, L.; Yang, C.; Pang, Q.; Ai, Q.; Chen, L.; Chen, M.; Li, G.; Yang, J.; Ma, Y. 885 nm LD end-pumped 22.7 W high beam quality electro-optical Q-switched Nd:YAG laser. *Laser Phys.* **2012**, *22*, 914–917. [[CrossRef](#)]
9. Liu, K.; Li, F.; Xu, H.; Wang, Z.; Zong, N.; Du, S.; Bo, Y.; Peng, Q.; Cui, D.; Xu, Z. High-power high-efficiency acousto-optically Q-switched rod Nd:YAG laser with 885 nm diode laser pumping. *Opt. Commun.* **2013**, *286*, 291–294. [[CrossRef](#)]
10. Wang, S.; Zhu, S.; Chen, Z.; Li, A.; Li, Z.; He, Q.; Yin, H. High average power, side-pumped passively Q-switched laser of 1064 nm by using composite crystal Nd:YAG/Cr⁴⁺:YAG/YAG. *J. Opt. UK* **2014**, *43*, 183–187. [[CrossRef](#)]
11. Maleki, A.; Moghtader dindarlu, M.H.; Saghafifar, H.; Kavosh Tehrani, M.; Soltanolkotabi, M.; Dehghan Baghi, M.; Maleki Ardestani, M.R. 57 mJ with 10 ns passively Q-switched diode pumped Nd:YAG laser using Cr⁴⁺:YAG crystal. *Opt. Quant. Electron.* **2016**, *48*, 48. [[CrossRef](#)]
12. Lee, H.C.; Chang, D.W.; Lee, E.J.; Yoon, H.W. High-energy, sub-nanosecond linearly polarized passively Q-switched MOPA laser system. *Opt. Laser Technol.* **2017**, *95*, 81–85. [[CrossRef](#)]
13. Ahmad, M.T.; Muhammad, A.R.; Zakaria, R.; Rahim, H.R.A.; Hamdan, K.S.; Yusof, H.H.M.; Arof, H.; Harun, S.W. Gold nanoparticle based saturable absorber for Q-switching in 1.5 μm laser application. *Laser Phys.* **2017**, *27*, 115101. [[CrossRef](#)]
14. Ahmad, M.T.; Muhammad, A.R.; Haris, H.; Rahim, H.R.A.; Zakaria, R.; Ahmad, H.; Harun, S.W. Q-switched Ytterbium doped fibre laser using gold nanoparticles saturable absorber fabricated by electron beam deposition. *Optik* **2019**, *182*, 241–248. [[CrossRef](#)]
15. Rizman, Z.I.; Rusdi, M.F.M.; Arof, H.; Latiff, A.A.; Apsari, R.S.; Harun, W. Tunable Q-switched erbium-doped fiber laser using gold nanoparticles saturable absorber. *Nonlinear Opt. Quantu.* **2019**, *50*, 293–301.
16. Zirngibl, M.; Stulz, L.W.; Stone, J.; Stone, J.; Digiovanni, D.; Hansen, P.B. 1.2 ps pulses from passively mode-locked laser diode pumped Er-doped fibre ring laser. *Electron. Letts.* **1991**, *27*, 1734–1735. [[CrossRef](#)]
17. Loh, W.H.; Atkinson, D.; Morkel, P.R.; Hopkinson, M.; Rivers, A.A.; Seeds, J.; Payne, D.N. Passively mode-locked Er³⁺ fiber laser using a semiconductor nonlinear mirror. *IEEE Photon. Technol. Lett.* **1993**, *5*, 35–37. [[CrossRef](#)]
18. Loh, W.H.; Atkinson, D.; Morkel, P.R.; Hopkinson, M.; Rivers, A.; Seeds, A.J.; Payne, D.N. All-solid-state subpicosecond passively mode locked erbium-doped fiber laser. *Appl. Phys. Lett.* **1993**, *63*, 4–6. [[CrossRef](#)]
19. Yu, H.; Chen, X.; Zhang, H.; Xu, X.; Hu, X.; Wang, Z.; Wang, J.; Zhuang, S.; Jiang, M. Large energy pulse generation modulated by graphene epitaxially grown on silicon carbide. *ACS Nano* **2010**, *4*, 7582–7586. [[CrossRef](#)] [[PubMed](#)]

20. Jiang, M.; Ren, Z.; Lu, B.; Guo, T.; Wan, L.; Zhang, Y.; Bai, J. Low-repetition-rate high-energy passively Q-switched Nd:YAG solid laser based on graphene saturable absorber operating at 1064nm. *Curr. Nanosci.* **2012**, *8*, 60–63. [[CrossRef](#)]
21. Lin, H.; Huang, X.; Liu, X.; Xu, Y. Passively Q-switched Nd:YAG laser with multilayer graphene as a saturable absorber. *J. Russ. Laser Res.* **2015**, *36*, 281–284. [[CrossRef](#)]
22. Evangelatos, C.; Bakopoulos, P.; Tsaknakis, G.; Papadopoulos, D.; Avdikos, G.; Papayannis, A.; Tzeremes, G. Continuous wave and passively Q-switched Nd:YAG laser with a multisegmented crystal diode-pumped at 885 nm. *Appl. Opt.* **2013**, *52*, 8795–8801. [[CrossRef](#)] [[PubMed](#)]
23. Li, X.; Zhou, Y.; Yan, R.; Ma, Y.; Chen, D.; Zhou, Z. A compact YAG/Nd:YAG/Cr:YAG Passively Q-switched pulse burst laser pumped by 885 nm laser diode. *J. Russ. Laser Res.* **2017**, *38*, 387–391. [[CrossRef](#)]